

Shape-Guided Diffusion with Inside-Outside Attention

Dong Huk Park^{1*}
Xihui Liu^{1,3†}

Grace Luo^{1*}
Maka Karalashvili⁴

Clayton Toste¹
Anna Rohrbach¹

Samaneh Azadi²
Trevor Darrell¹

¹UC Berkeley

²Meta AI

³The University of Hong Kong

⁴BMW Group

{dong.huk.park, graceluo}@berkeley.edu

* Denotes equal contribution.



Figure 1: We demonstrate the importance of using an explicit shape when performing a local edit on a real image. Prior work (P2P [8]) has difficulty preserving the source object’s shape, even when adapted for local editing (P2P + Shape). We propose *Shape-Guided Diffusion*, a training-free method that uses a novel *Inside-Outside Attention* mechanism to delineate which spatial regions are object vs. background and ensure that edits are localized to the correct region. Our method can be provided an object mask as input or infer a mask from text, as is shown in the above example.

Abstract

When manipulating an object, existing text-to-image diffusion models often ignore the shape of the object and generate content that is incorrectly scaled, cut off, or replaced with background content. We propose a training-free method, *Shape-Guided Diffusion*, that modifies pretrained diffusion models to be sensitive to shape input specified by a user or automatically inferred from text. We use a novel *Inside-Outside Attention* mechanism during the inversion and generation process to apply this shape constraint to the cross- and self-attention maps. Our mechanism designates which spatial region is the object (inside) vs. background (outside) then associates edits specified by text prompts to the correct region. We demonstrate the efficacy of our method on the shape-guided editing task, where the model must replace an object according to a text prompt and object

mask. We curate a new *ShapePrompts* benchmark derived from MS-COCO and achieve SOTA results in shape faithfulness without a degradation in text alignment or image realism according to both automatic metrics and annotator ratings. Our data and code will be made available at <https://shape-guided-diffusion.github.io>.

1. Introduction

Recent large-scale diffusion models [27, 28, 25], have significantly improved the realism of text-conditional image synthesis and its faithfulness to the input prompt. However, there is a limit to what can be expressed via language. For example, users must perform extensive prompt tuning to achieve a desired silhouette or select one object instance out of many, when their intent could be more easily specified with an object mask. Whether this mask is user specified or implicitly inferred, prior work in image editing is

[†]This work was done when Xihui Liu was a postdoc at UC Berkeley.

often insensitive to the source object’s shape and violates affordances (e.g., producing a dog with missing limbs or a truck with a missing cargo container) or interactions (e.g., producing a boat with an inconsistent reflection) that were present in the original image (see Figure 1). Enabling text-to-image diffusion models to respect shape guidance is especially beneficial for applications like anonymization, targeted ads customization, or synthetic data generation. Thus, we consider the task of *shape-guided editing*, where a real image, text prompt, and object mask are fed to a pre-trained text-to-image diffusion model to synthesize a new object faithful to the the text prompt and the mask’s shape.

Our method is motivated by the observation that diffusion models often contain spurious attentions that weakly associate object and background pixels. To overcome this issue, we delineate the object (inside) and background (outside) with a novel Inside-Outside Attention mechanism that removes spurious attentions during both the inversion and generation process. This mechanism modifies the cross- and self-attention maps such that a token or pixel referring to the object is constrained to attend to pixels inside the shape, and vice versa.

To summarize, our contributions include the following:

- (1) We identify a limitation in prior image editing methods where the shape of the original object is not preserved and provide empirical insights on why this issue exists.
- (2) Unlike existing mask-based editing adaptations (e.g., copying the background or finetuning the model to use mask input), we introduce a training-free mechanism that applies a shape constraint on the attention maps at inference time. To the best of our knowledge, we are the first work to explore *constraining* attention maps during inversion, which allows us to discover inverted noise that better preserves shape information from a real image.
- (3) Our method achieves SOTA results in shape faithfulness on our MS-COCO ShapePrompts benchmark, and is rated by annotators as the best editing method 2.7x more frequently than the most competitive baseline. We demonstrate diverse editing capabilities such as object edits, background edits, and simultaneous inside-outside edits.

2. Related Work

Diffusion Models Diffusion models [30] have had remarkable success in image synthesis. They define a Markov chain of diffusion steps that slowly adds random noise to data then learn a model that can reverse the diffusion process to construct desired data samples from the noise. Variants of diffusion models include Denoising Diffusion Probabilistic Models (DDPM) [9], Denoising Diffusion Implicit Models (DDIM) [31], and score-based models [32]. Classifier guidance [5] and classifier-free guidance [10] have been investigated for conditional image synthesis. Recently, diffusion models [26, 21, 27, 28] have shown impressive per-

Approach	(a) Guidance	(b) Attn Map	(c) Inversion
SDEdit [18]	edit prompt	N/A	N
P2P [8]	src prompt, edit prompt	Copy	Y
InstructPix2Pix* [2]	edit instruction	Copy	N
NTI* [20]	src prompt, edit prompt	Copy	Y
PNP* [36]	src prompt, edit prompt	Copy	Y
Ours	src prompt, edit prompt, shape	Constrain	Y

Table 1: A conceptual comparison of our work vs. structure preserving methods. We compare against SDEdit and P2P in a large-scale evaluation, whereas for concurrent works (denoted by *) we include examples in the Supplemental.

formance on text-guided image synthesis. Our work focuses on adapting these diffusion models towards text-guided local editing according to a text prompt and object mask.

Global and Local Image Editing Researchers have proposed a variety of methods to extend generative models towards image editing. For text-guided global editing, StyleCLIP [23] adapts StyleGAN [12] and DiffusionCLIP [14] adapts diffusion models to edit entire images according to a text prompt using CLIP [24]. Blended Diffusion [1] proposes a method for local editing constrained to a mask by copying an appropriately noised version of the source image’s background at each diffusion timestep. While this “copy background” technique can be generally combined with other methods to enable local editing in diffusion models, we demonstrate that this method alone is insufficient for preserving object shape, and we further improve shape faithfulness with our proposed method.

Structure Preserving Image Editing Aside from global and local image editing, there also exists work in structure preserving image editing. These works aim to maintain structure, including the position or pose of the object to be edited. To achieve structure preservation, some works copy random seeds [39], finetune model weights [37, 13], copy features and self-attention maps [36], or condition on a partially noised version of the source image [18]. Prompt-to-Prompt (P2P) [8] copies cross-attention maps from the source to target image, and follow up works concurrent to ours improve its performance on real image editing [20, 2].

We present a conceptual comparison of our work vs. a few structure preserving works with open source code in Table 1 (see additional examples in the Supplemental). (a) While these methods are often able to produce a background that looks similar to that of the source image, they struggle to perform a local edit where the background is not disturbed because they lack shape as an explicit form of guidance. (b) Unlike prior work that leverages attention maps for image editing, we do not *copy* these attention maps but rather *constrain* them to be sensitive to shape. While directly copied attention maps are noisy and entangle changes in object and background pixels, our constrained attention maps spatially localize these changes, which allows us to perform shape-guided edits (see Figure 4). (c) Although P2P demonstrates success in structure consistency when

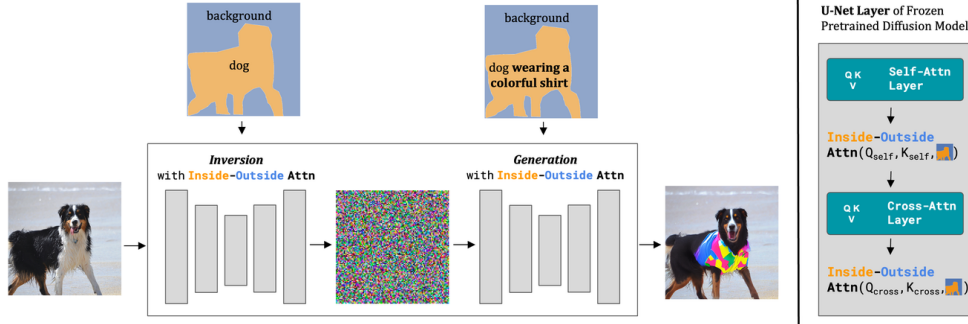


Figure 2: Shape-Guided Diffusion. Our method takes a real image, source prompt (“dog”), edit prompt (“dog wearing a colorful shirt”), as well as an optional object mask (inferred from the source prompt if not provided), and outputs an edited image. Left: we modify a frozen pretrained text-to-image diffusion model during both the inversion and generation processes. Right: we show a detailed view of one layer in the U-Net, where Inside-Outside Attention constrains the self- and cross-attention maps according to the mask.

generating multiple synthetic images, it has difficulty preserving the structure of a real image. It shows initial results for real image editing using DDIM inversion [31, 5], a deterministic technique that inverts a real image into noise that would reconstruct the image when fed to the diffusion model for generation. While the inverted noise retains some structure information, combining inversion with classifier-free guidance often causes a drift issue where it is difficult to simultaneously preserve the structure and respect the text prompt. As seen in Figure 4, we demonstrate that our shape constraint on the attention maps is able to mitigate this drift issue, which is also explored in the concurrent work Null Text Inversion [20] that instead proposes test-time optimization of null embeddings.

Image Inpainting Image inpainting is the task of generating missing regions of an image for object removal, image restoration, etc. Researchers have proposed dilated convolution [11], partial convolution [16], gated convolution [42], contextual attention [41], and co-modulation [44] for GAN-based image inpainting. Lugmayr *et al.* [17] recently proposed a diffusion-based model for free-form image inpainting. There exist variants of GLIDE [21] and Stable Diffusion [27, 19] finetuned for text-conditional inpainting. However, these methods were trained with free-form masks without semantic meaning, where infilling the mask with background is reasonable and even encouraged. There exist a few training-based methods that use object masks, none of which are publicly available. Make-a-Scene [6] trained an auto-regressive transformer conditioned on full segmentation maps of a scene. Shape-guided Object Inpainting [43] trained a GAN and Imagen Editor [38] trained Imagen [28] with object masks for inpainting. In contrast, we apply our model on top of an open-source text-to-image diffusion model at inference time. Because our method is training-free, it is more flexible and can be applied towards tasks beyond object editing, such as background editing or simultaneous inside-outside editing, as discussed in Sec. 5.2.

3. Shape-Guided Diffusion

We present Shape-Guided Diffusion, a *training-free* method that enables a pretrained text-to-image diffusion model to respect shape guidance. Our goal is to locally edit image x_{src} given text prompts \mathcal{P}_{src} and \mathcal{P}_{edit} and optional object mask m (inferred from \mathcal{P}_{src} if not provided), so that edited image x_{edit} is faithful to both \mathcal{P}_{edit} and m . We introduce Inside-Outside Attention to explicitly constrain the cross- and self-attention maps during both the inversion (image to noise) and generation (noise to image) processes. An overview of our method can be found in Figure 2.

We build upon Stable Diffusion (SD), a Latent Diffusion Model (LDM) [27] that operates in low-resolution latent space. LDM latent space is a perceptually equivalent downsampled version of image space, meaning we are able to apply Inside-Outside Attention in latent space via downsampled object masks. For the rest of this paper, when we denote “pixel”, “image”, or “noise”, we are referring to these concepts in LDM latent space.

3.1. Inside-Outside Attention

LDMs contain both cross-attention layers used to produce a spatial attention map for each textual token and self-attention layers used to produce a spatial attention map for each pixel. We postulate that prior methods often fail because of spurious attentions – attentions that seek to edit the object compete with those that seek to preserve the background because they are not well localized (see Figure 4). Hence, we manipulate the cross-attention map such that the inside tokens are responsible for editing a distinct, non-overlapping spatial region compared with the outside tokens (e.g., “dog”, “shirt”, etc. may only edit the dog and “background” may only edit the remaining scene). Since self-attention layers heavily influence how pixels are grouped to form coherent objects, we apply a similar manipulation to the self-attention map to further ensure that the desired object is contained within the boundaries of the input mask.

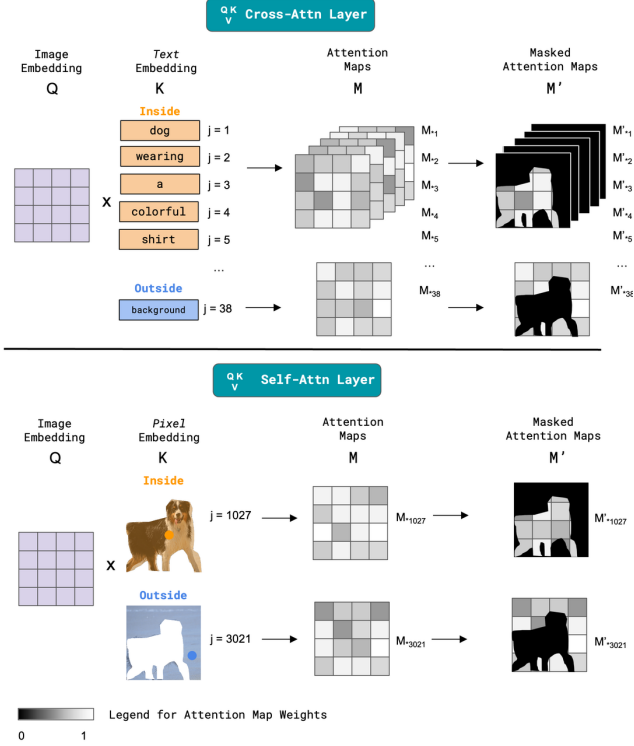


Figure 3: Inside-Outside Attention. We modify the attention maps from both the cross-attention and self-attention layers. Here j refers to token/pixel indices and M_{*j} denotes the attention map corresponding to the j -th index. Top: in the cross-attention layer depending on whether the text embedding refers to the inside or outside the object, we constrain the attention map M according to the object mask or the inverted object mask to produce M' . Bottom: in the self-attention layer we perform a similar operation on the inside and outside pixel embeddings.

An overview of Inside-Outside Attention is given in Figure 3 and our algorithm is defined as follows (also see Alg. 1). For one forward pass at each timestep during inversion or generation, we go through all layers of the diffusion model DM and manipulate the cross- and self-attention maps M . We denote the dimensions of M as $\mathbb{R}^{HW \times d_\tau}$ and $\mathbb{R}^{HW \times HW}$ for each cross- and self-attention map, respectively, where H is the image height, W is the image width, HW is the number of pixels in the flattened image, and d_τ is the number of tokens. We also downsample m according to the resolution of the cross- or self-attention layer. For the cross-attention map, we determine column indices J_{in} and J_{out} based on whether the token refers to the object or the background. For the self-attention map, we determine column indices J_{in} and J_{out} based on whether the pixel belongs inside or outside the object as defined by mask m . Finally, we compute the new constrained attention maps $M'_{*j_{in}} = \{M_{*j_{in}} \odot m \mid \forall j_{in} \in J_{in}\}$ and $M'_{*j_{out}} = \{M_{*j_{out}} \odot (1 - m) \mid \forall j_{out} \in J_{out}\}$.

Algorithm 1 Inside-Outside Attention

Input: A diffusion model DM , a binary object mask m , a prompt \mathcal{P} .

Output: An edited diffusion model where the attention maps M are masked according to m and \mathcal{P} for one forward pass.

```

1: for all  $l \in \text{layers}(DM)$  do
2:   if  $\text{type}(l)$  is CrossAttention
3:      $J_{in} \leftarrow \{j \mid j\text{th token refers to object}\}$ 
4:      $J_{out} \leftarrow \{j \mid j\text{th token refers to background}\}$ 
5:   elif  $\text{type}(l)$  is SelfAttention
6:      $J_{in} \leftarrow \{j \mid j\text{th pixel belongs inside object}\}$ 
7:      $J_{out} \leftarrow \{j \mid j\text{th pixel belongs outside object}\}$ 
8:      $M'_{*j_{in}} = M_{*j_{in}} \odot m \quad \forall j_{in} \in J_{in}$ 
9:      $M'_{*j_{out}} = M_{*j_{out}} \odot (1 - m) \quad \forall j_{out} \in J_{out}$ 
10: end for

```

3.2. Inside-Outside Inversion

To edit real images, we use DDIM inversion [31, 21] to convert the source image to inverted noise. However, we observe that using inversion with a text-to-image diffusion model often results in a shape-text faithfulness tradeoff. Nonzero levels of classifier-free guidance can completely destroy information about the source object (see bottom row of Figure 4). We propose applying Inside-Outside Attention to mitigate this trade-off. Similar to how prior work can associate tokens to *entire images* [7, 37], with Inside-Outside Attention we can associate tokens to *specific spatial regions*. As such, if the token remains the same its associated region should remain the same (e.g., “dog” and “background” in the reconstruction setting) and if it changes its associated region should change (e.g., “dog” in the editing setting) without affecting other regions. While without our method (bottom) the inverted noise is able to retain some information about the real image – the checkerboard pattern on the chair is converted to flowers or polka dots in the bottom row – with our method (top) the edited image is able to retain the full chair. We also depict the cross-attention map for “dog”, where without our method the attention map weakly includes the background and with our method the map is localized to the dog.

3.3. Method Summary

In summary, we make the observation that object shape can be better preserved if spurious attentions are removed, and we propose the novel inference-time mechanism Inside-Outside Attention. Our method Shape-Guided Diffusion uses Inside-Outside Attention to constrain the attention maps during both inversion and generation, which we depict in Figure 2. The Shape-Guided Diffusion algorithm can be defined as follows (also see Alg. 2).

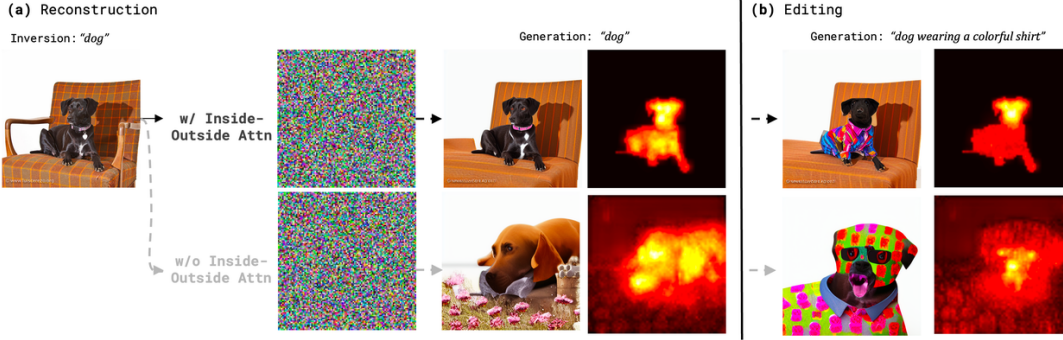


Figure 4: Spurious attentions and classifier-free guidance limits shape preservation. Inside-Outside Attention (top) preserves the shape relationship between the object and background by associating tokens to specific spatial regions. We demonstrate this property when reconstructing (left) and editing (right) a real image with classifier-free guidance. We also depict the cross attention map for the token “dog” averaged all attention heads and timesteps.

Algorithm 2 Shape-Guided Diffusion

Input: A diffusion model DM with autoencoder \mathcal{E}, \mathcal{D} , real image x_{src} , a source prompt \mathcal{P}_{src} , an edit prompt \mathcal{P}_{edit} , and either a binary object mask m or a shape inference function $\text{InferShape}(\cdot)$.

Hyperparameters: Classifier-free guidance scale w_g .

Output: An edited image x_{edit} that differs from x_{src} only within the mask region m .

```

1: if  $m$  is not provided then
2:    $m \leftarrow \text{InferShape}(x_{src}, \mathcal{P}_{src})$ 
3: end if
4:  $[\bar{z}_0, \dots, \bar{z}_T] \sim \text{InsideOutsideInv}(z|\mathcal{E}(x_{src}), \mathcal{P}_{src}, m, DM)$ 
5:  $z_T \leftarrow \bar{z}_T$ 
6: for all  $t$  from  $T$  to 1 do
7:    $\text{InsideOutsideAttention}(DM, \mathcal{P}_{edit}, m)$ 
8:    $z_{cond} \leftarrow DM(z_t, \mathcal{P}_{edit})$ 
9:    $z_{uncond} \leftarrow DM(z_t, \emptyset)$ 
10:   $z_{t-1} \leftarrow z_{cond} + w_g * (z_{cond} - z_{uncond})$ 
11:   $z_{t-1} \leftarrow z_{t-1} \odot m + \bar{z}_{t-1} \odot (1 - m)$ 
12: end for
13:  $x_{edit} \leftarrow \mathcal{D}(z_0)$ 

```

If the mask is not provided, we use the shape inference function $\text{InferShape}(\cdot)$ to identify \mathcal{P}_{src} in the image. For our experiments we use an off-the-shelf segmentation model [4], but any method for textual grounding could also be used with our method. We run Inside-Outside Inversion on the conditional diffusion model driven by the prompt \mathcal{P}_{src} (e.g., “dog”) to get inverted noise \bar{z}_T . We then set our initial noise z_T to \bar{z}_T . For each sampling step, we apply Inside-Outside Attention for both the conditional and unconditional diffusion models using mask m and \mathcal{P}_{edit} (e.g., “dog wearing a colorful shirt”).

We mix the predictions of both models using the original formulation of Ho *et al.* [9], which applies classifier-free guidance to the conditional prediction (Line 10, Alg. 2). In early experiments we found this design choice leads to higher text alignment without a loss in other metrics. Fi-

nally, we copy the real image’s background found during the inversion process $\bar{z}_{t-1} \cdot m$ to form the edited image prediction z_{t-1} . This ensures the edited image x_{edit} and the original image x_{src} only differ within the mask region m .

4. MS-COCO ShapePrompts

Benchmark We evaluate our approach on MS-COCO images [15]. We filter for object masks with an area between [2%, 50%] of the image, following prior work in image inpainting [34]. Our test set derived from MS-COCO val 2017 contains 1,149 object masks spanning 10 categories covering animal, vehicle, food, and sports classes. We create a validation set with 1,000 object masks in the same fashion derived from MS-COCO train 2017. For each category we design a few prompts that add clothing or accessories (e.g., “floral shirt” or “sunglasses”), manipulate color (e.g., “iridescent”, “with spray paint graffiti”), switch material (“lego”, “paper”), or specify rare subcategories (“spotted leopard cat”, “tortilla wrapped sandwich”). More information about the prompts can be found in the Supplemental.

Metrics Since we aim to synthesize an image faithful to the input shape, we use mean Intersection over Union (mIoU) as a metric. Specifically, we compute the proportion of pixels within the masked region correctly synthesized as the desired object class, as determined by a segmentation model [4] trained on COCO-Stuff [3]. Since animal object masks are particularly fine-grained, and mIoU does not capture a full picture of degenerate cases (e.g., if the edit replaces a cat’s full body with a cat’s head), we also compute a keypoint-weighted mIoU (KW-mIoU) for the animal classes. Specifically, we weight each sample’s mIoU by the percentage of correct keypoints when comparing the source vs. edited image, as determined by an animal keypoint detection model [40]. We also report FID scores as a metric for image realism, which measures the similarity of the distributions of real and synthetic images using the features of an Inception network [35, 22]. Finally, we report CLIP [24]



Figure 5: Comparison to prior work. We compare our results with Blended Diffusion [1], SD-Inpaint [19], SDEdit [18], and P2P [8] with the MS-COCO image and instance mask for reference. Our method is able to generate realistic edits that are faithful to both the input shape and text prompt. + Shape denotes a variant of the structure preserving method adapted for local image editing using the “copy background” method from [1].

scores as a metric for image-text alignment, which measures the similarity of the text prompt and synthetic image using the features of a large pretrained image-text model. More information on metrics can be found in the Supplemental.

5. Experiments

In Sec. 5.1 we evaluate our method on the shape-guided editing task where it must replace an object given a (real image, text prompt, object mask) triplet from MS-COCO ShapePrompts. We also evaluate on the same task with masks inferred from the text and ablate the use of our Inside-Outside Attention mechanism. In Sec. 5.2 we present additional results beyond object editing.

Baselines For our baselines, we compare against the lo-

cal image editing method Blended Diffusion [1], the inpainting method SD-Inpaint [19], and the structure preserving methods SDEdit [18] and P2P [8]. Blended Diffusion, built on top of a Guided Diffusion [5] backbone, uses mask input by copying the source image’s background at each timestep and text input by applying classifier guidance with CLIP [24]. SD-Inpaint, built on top of a Stable Diffusion [27] backbone, finetunes the model with an extra U-Net channel to use mask input and applies classifier-free guidance to use text input. SDEdit partially noises then denoises the source image and P2P copies cross attention maps to preserve structure, and they apply classifier-free guidance to use text input. For the structure preserving methods we use implementations built on top of a Stable Diffusion back-

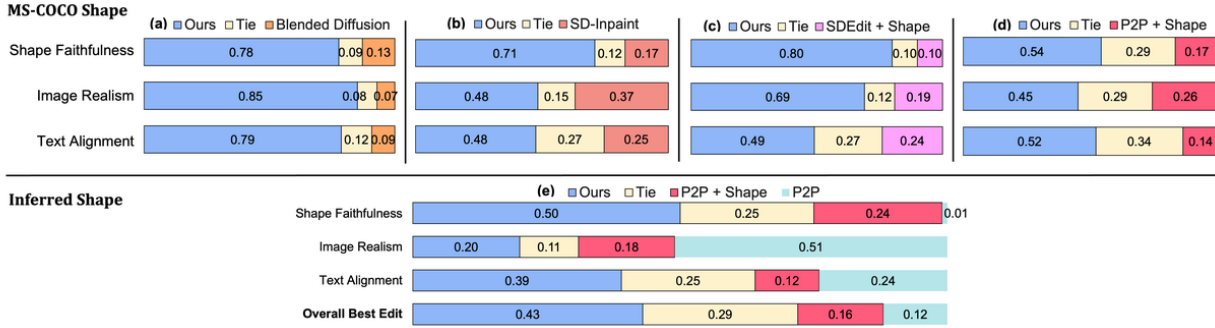


Figure 6: Annotator evaluation on MS-COCO ShapePrompts (100-sample subset of test set). Columns (a, b, c, d): we asked people to rate edits performed by our method vs. a baseline, where the two edits were presented as anonymized and in randomized order. Rows (shape faithfulness, image realism, text alignment): annotators selected the superior edit along these three axes. Each bar denotes the percentage of samples where the superior edit was “Ours”, “Tie”, or a baseline. In (e) we use the same procedure, except we presented three anonymized edits, ours vs. two baselines. Annotators were additionally asked to select the “overall best edit.” We provide further details in the Supplemental.

Approach	KW-mIoU (\uparrow)	mIoU (\uparrow)	FID (\downarrow)	CLIP (\uparrow)
Real Images	83.3	76.3	-	0.15
MS-COCO Shape				
Blended Diffusion [1]	23.3	41.8	46.2	0.20
SD-Inpaint [19]	38.5	51.7	43.7	0.19
SDEdit + Shape [18]	31.0	49.9	45.1	0.21
P2P + Shape [8]	46.9	63.3	39.6	0.20
Ours (w/o IOA)	43.8	55.3	41.5	0.21
Ours	53.3	63.6	40.2	0.21
Inferred Shape				
P2P [8]	24.2	64.6	97.5	0.26
P2P + Shape [8]	37.7	54.0	51.1	0.21
Ours (w/o IOA)	33.0	46.0	56.8	0.22
Ours	43.0	54.9	49.5	0.22

Table 2: Automatic evaluation on MS-COCO ShapePrompts (test set). MS-COCO Shape uses instance masks provided by MS-COCO, and Inferred Shape uses masks inferred from the text. Ours w/o IOA denotes our method without Inside-Outside Attention.

bone, and in some experiments we adapt them to use mask input by applying the “copy background” method from [1].

Experimental Setup For all baselines we use the default hyperparameters provided by their respective repositories. For sampling we use a standard DDIM scheduler for 50 inversion and generation steps. When using Inside-Outside Attention on cross-attention layers, we evenly divide the maximum number of text tokens excluding the `<bos>` token, resulting in 38 “inside” tokens and 38 “outside” tokens. The attentions for the `<bos>` token are zeroed out.

5.1. Comparison to Prior Work

MS-COCO Shape We first experiment with instance-level masks provided by MS-COCO as our shape guidance. In Figure 5, we depict real images (first row) and edits made by Blended Diffusion (second row), SD-Inpaint (third row), and SDEdit + Shape (fourth row), P2P + Shape (fifth row), Ours (sixth row). Prior works demonstrate a variety of failure modes in shape-guided editing, where an object

may be transformed into a new shape, removed completely, severely downscaled, or fail to respect the text prompt. On the other hand, our method is able to simultaneously respect the shape and the prompt without a compromise in image realism. As seen in Table 2, our method outperforms the local editing and inpainting baselines [1, 19] across the board, with at least a 15 point improvement in KW-mIoU. Comparing with the structure preserving baselines [18, 8], we achieve at least a 6 point improvement in KW-mIoU with comparable FID and CLIP scores. Intuitively, the baselines have trouble achieving shape faithfulness because “copy background” only provides shape signal based on how realistic the visual output looks at each timestep – the diffusion model attempts to rectify its edits based on how well it blends with the copied background. In Figure 7 we demonstrate this shape signal is weak in early diffusion timesteps where the output looks similar to pure noise, meaning that the model can irrecoverably produce an object with the incorrect scale or pose. Our Inside-Outside attention mechanism provides much stronger shape signal in early timesteps, where we enforce the location and scale of the object via the attention constraint.

We also conducted an evaluation with annotator ratings. We created four evaluations corresponding to each baseline, each of which contained 100 samples comparing an edit made by our method vs. the baseline in an anonymized and randomized fashion. For each sample, we asked five people to select the superior edit along the axes of shape faithfulness, image realism, and text alignment. As seen in the top row of Figure 6, annotators confirm that our method outperforms the baselines in shape faithfulness, with our method selected as superior at least 54% of the time (3.2x the most competitive baseline P2P + Shape). For image realism and text alignment, our method was selected as superior at least 48% of the time (1.3x and 1.9x the most competitive baseline SD-Inpaint).

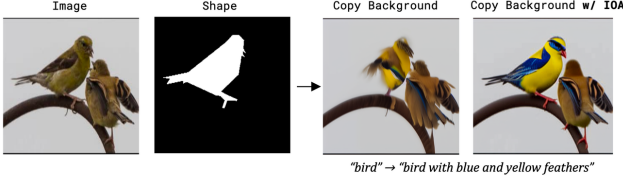


Figure 7: Shape signal from “copy background” is weak in early timesteps. In both examples we only use shape guidance in the first half of generation, where Inside-Outside Attention (w/ IOA) is able to provide stronger shape signal.

Inferred Shape Next, we demonstrate that our method also works on automatically inferred masks, which encompass a variety of challenging cases, such as reflections or multiple overlapping instances (Figure 1). We compare against our most competitive baseline, vanilla P2P and P2P adapted for local image editing using the inferred mask (P2P + Shape). P2P often produces edits that look nothing like the source image (see Figure 1), explaining how it has the worst FID scores in Table 2 (its distribution of synthetic images is significantly different than the real images) but the best image realism ratings in Figure 6. In a similar fashion, it achieves a better CLIP score but worse text alignment rating than our method because it is easier to align with the prompt if significantly deviating from the source image. As a result, P2P is rated as the worst overall image *editing* method, as seen in the bottom row of Figure 6. In contrast, our method is rated as the best edit for 43% of samples, 2.7x more than the most competitive baseline P2P + Shape.

Ablations In Table 2 we ablate our method without Inside-Outside Attention (Ours w/o IOA) and with Inside-Outside Attention (Ours). We demonstrate that the mechanism is a critical component of our method, providing a 9.5 point and 10 point increase in KW-mIoU in the MS-COCO Shape and Inferred Shape settings respectively. Ours w/o IOA performs better than all baselines on all metrics, except P2P + Shape (only P2P and our method use inversion), demonstrating how DDIM inversion is another critical component. In the Supplemental we also ablate the use of DDIM inversion, guidance scale hyperparameters, and the use of a soft vs. hard shape constraint on the self-attention maps.

5.2. Additional Editing Results

In Figure 8, we demonstrate additional capabilities of our method beyond object editing. (a) Our method is able to perform both intra- and inter- class edits on the same image, for example editing a cow to wear “gold and diamond chains” or transform into a “sheep.” (b) Our method is able to perform outside edits, whether it is a background “at sunset” or “in front of the Eiffel Tower in Paris.” Interestingly, our method sometimes maintains structures from the real image, for example transforming the cabinet into a landmass in both edited images. (c) Our method is able to

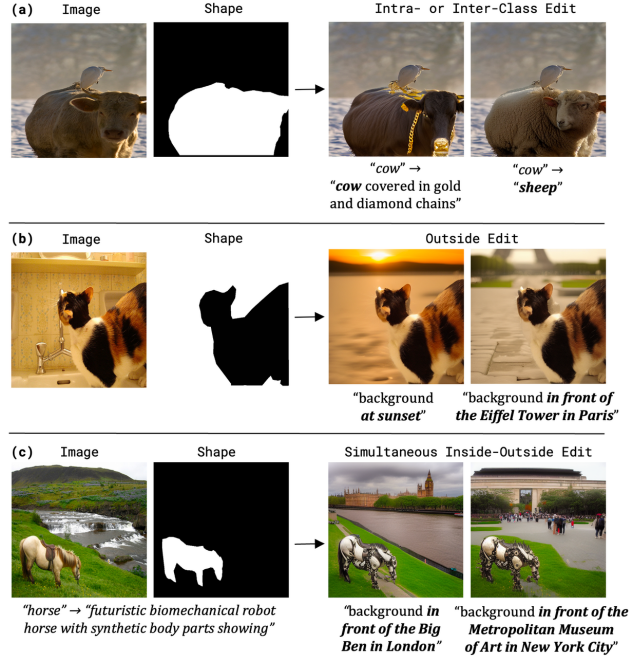


Figure 8: Additional editing results. Our method can perform intra- or inter-class edits on the same image, outside edits, and simultaneous inside-outside edits.

perform simultaneous edits with one prompt for the inside region (“...robot horse...”) and another for the outside region (“...Big Ben...” or “...Metropolitan Museum of Art...”). Since our method delineates edits on the object vs. background, although every pixel in the image is transformed we can maintain the object-background relation from the source scene (e.g., the horse grazing). In contrast, it is not obvious how to adapt structure preserving methods for this simultaneous editing setting, since with “copy background” they require one region (e.g., the background) to remain identical to the source image to enforce locality.

6. Conclusion

In this work, we present the usefulness of an explicit shape for local edits on real images. We show that prior work in local editing, structure preserving editing, and inpainting often fail to respect shape. To alleviate this issue, we propose Shape-Guided Diffusion, a training-free method that uses a novel Inside-Outside Attention mechanism during both the inversion and generation process, which localizes object vs. background edits. We evaluate our method on our newly proposed MS-COCO ShapePrompts benchmark on the shape-guided editing task, where the goal is to edit an object given an input mask and text prompt. We show that our method significantly outperforms the baselines in shape faithfulness without a degradation in text alignment or image realism when using either precise MS-COCO instance masks or masks inferred from the text.

Acknowledgements. This work was supported in part by DoD including DARPA’s SemaFor, PTG and/or LwLL programs, as well as BAIR’s industrial alliance programs.

References

- [1] Omri Avrahami, Dani Lischinski, and Ohad Fried. Blended diffusion for text-driven editing of natural images. In *CVPR*, 2022. 2, 6, 7, 11, 13
- [2] Tim Brooks, Aleksander Holynski, and Alexei A. Efros. Instructpix2pix: Learning to follow image editing instructions. *arXiv preprint arXiv:2211.09800*, November 2022. 2, 15
- [3] Holger Caesar, Jasper Uijlings, and Vittorio Ferrari. Coco-stuff: Thing and stuff classes in context. In *CVPR*, 2018. 5
- [4] Bowen Cheng, Alexander G. Schwing, and Alexander Kirillov. Per-pixel classification is not all you need for semantic segmentation. In *NeurIPS*, 2021. 5, 11, 16
- [5] Prafulla Dhariwal and Alexander Nichol. Diffusion models beat gans on image synthesis. In *NeurIPS*, 2021. 2, 3, 6
- [6] Oran Gafni, Adam Polyak, Oron Ashual, Shelly Sheynin, Devi Parikh, and Yaniv Taigman. Make-a-scene: Scene-based text-to-image generation with human priors. *arXiv preprint arXiv:2203.13131*, 2022. 3
- [7] Rinon Gal, Yuval Alaluf, Yuval Atzmon, Or Patashnik, Amit H Bermano, Gal Chechik, and Daniel Cohen-Or. An image is worth one word: Personalizing text-to-image generation using textual inversion. *arXiv preprint arXiv:2208.01618*, 2022. 4
- [8] Amir Hertz, Ron Mokady, Jay Tenenbaum, Kfir Aberman, Yael Pritch, and Daniel Cohen-Or. Prompt-to-prompt image editing with cross attention control. *arXiv preprint arXiv:2208.01626*, 2022. 1, 2, 6, 7, 11, 12, 13, 14, 15, 20
- [9] Jonathan Ho, Ajay Jain, and Pieter Abbeel. Denoising diffusion probabilistic models. In *NeurIPS*, 2020. 2, 5
- [10] Jonathan Ho and Tim Salimans. Classifier-free diffusion guidance. *arXiv preprint arXiv:2207.12598*, 2022. 2
- [11] Satoshi Iizuka, Edgar Simo-Serra, and Hiroshi Ishikawa. Globally and locally consistent image completion. *ACM Transactions on Graphics (ToG)*, 36(4):1–14, 2017. 3
- [12] Tero Karras, Samuli Laine, and Timo Aila. A style-based generator architecture for generative adversarial networks. In *CVPR*, 2019. 2
- [13] Bahjat Kawar, Shiran Zada, Oran Lang, Omer Tov, Huiwen Chang, Tali Dekel, Inbar Mosseri, and Michal Irani. Imagic: Text-based real image editing with diffusion models. *arXiv preprint arXiv:2210.09276*, 2022. 2
- [14] Gwanghyun Kim, Taesung Kwon, and Jong Chul Ye. Diffusionclip: Text-guided diffusion models for robust image manipulation. In *CVPR*, 2022. 2
- [15] Tsung-Yi Lin, Michael Maire, Serge Belongie, Lubomir Bourdev, Ross Girshick, James Hays, Pietro Perona, Deva Ramanan, C. Lawrence Zitnick, and Piotr Dollár. Microsoft coco: Common objects in context. In *ECCV*, 2014. 5
- [16] Guilin Liu, Fitsum A Reda, Kevin J Shih, Ting-Chun Wang, Andrew Tao, and Bryan Catanzaro. Image inpainting for irregular holes using partial convolutions. In *ECCV*, 2018. 3
- [17] Andreas Lugmayr, Martin Danelljan, Andres Romero, Fisher Yu, Radu Timofte, and Luc Van Gool. Repaint: Inpainting using denoising diffusion probabilistic models. In *CVPR*, 2022. 3
- [18] Chenlin Meng, Yutong He, Yang Song, Jiaming Song, Jianjun Wu, Jun-Yan Zhu, and Stefano Ermon. SDEdit: Guided image synthesis and editing with stochastic differential equations. In *International Conference on Learning Representations*, 2022. 2, 6, 7
- [19] Runway ML. Stable diffusion inpainting. <https://huggingface.co/runwayml/stable-diffusion-inpainting>, 2022. 3, 6, 7
- [20] Ron Mokady, Amir Hertz, Kfir Aberman, Yael Pritch, and Daniel Cohen-Or. Null-text inversion for editing real images using guided diffusion models. *arXiv preprint arXiv:2211.09794*, 2022. 2, 3, 15
- [21] Alex Nichol, Prafulla Dhariwal, Aditya Ramesh, Pranav Shyam, Pamela Mishkin, Bob McGrew, Ilya Sutskever, and Mark Chen. Glide: Towards photorealistic image generation and editing with text-guided diffusion models. In *ICML*, 2022. 2, 3, 4
- [22] Gaurav Parmar, Richard Zhang, and Jun-Yan Zhu. On aliased resizing and surprising subtleties in gan evaluation. In *CVPR*, 2022. 5
- [23] Or Patashnik, Zongze Wu, Eli Shechtman, Daniel Cohen-Or, and Dani Lischinski. Styleclip: Text-driven manipulation of stylegan imagery. In *ICCV*, 2021. 2
- [24] Alec Radford, Jong Wook Kim, Chris Hallacy, Aditya Ramesh, Gabriel Goh, Sandhini Agarwal, Girish Sastry, Amanda Askell, Pamela Mishkin, Jack Clark, et al. Learning transferable visual models from natural language supervision. In *ICML*, 2021. 2, 5, 6
- [25] Aditya Ramesh, Prafulla Dhariwal, Alex Nichol, Casey Chu, and Mark Chen. Hierarchical text-conditional image generation with clip latents. *arXiv preprint arXiv:2204.06125*, 2022. 1
- [26] Aditya Ramesh, Mikhail Pavlov, Gabriel Goh, Scott Gray, Chelsea Voss, Alec Radford, Mark Chen, and Ilya Sutskever. Zero-shot text-to-image generation. In *ICML*, 2021. 2
- [27] Robin Rombach, Andreas Blattmann, Dominik Lorenz, Patrick Esser, and Björn Ommer. High-resolution image synthesis with latent diffusion models. In *CVPR*, 2022. 1, 2, 3, 6
- [28] Chitwan Saharia, William Chan, Saurabh Saxena, Lala Li, Jay Whang, Emily Denton, Seyed Kamyar Seyed Ghasemipour, Burcu Karagol Ayan, S Sara Mahdavi, Rapha Gontijo Lopes, et al. Photorealistic text-to-image diffusion models with deep language understanding. *arXiv preprint arXiv:2205.11487*, 2022. 1, 2, 3
- [29] Sharif Shameem. Lexica. <https://lexica.art/>, 2022. 11
- [30] Jascha Sohl-Dickstein, Eric Weiss, Niru Maheswaranathan, and Surya Ganguli. Deep unsupervised learning using nonequilibrium thermodynamics. In *ICML*, 2015. 2
- [31] Jiaming Song, Chenlin Meng, and Stefano Ermon. Denoising diffusion implicit models. In *ICLR*, 2021. 2, 3, 4

- [32] Yang Song, Jascha Sohl-Dickstein, Diederik P Kingma, Abhishek Kumar, Stefano Ermon, and Ben Poole. Score-based generative modeling through stochastic differential equations. In *ICLR*, 2021. 2
- [33] Ke Sun, Bin Xiao, Dong Liu, and Jingdong Wang. Deep high-resolution representation learning for human pose estimation. In *Proceedings of the IEEE/CVF conference on computer vision and pattern recognition*, pages 5693–5703, 2019. 12
- [34] Roman Suvorov, Elizaveta Logacheva, Anton Mashikhin, Anastasia Remizova, Arsenii Ashukha, Aleksei Silvestrov, Naejin Kong, Harshith Goka, Kiwoong Park, and Victor Lempitsky. Resolution-robust large mask inpainting with fourier convolutions. *arXiv preprint arXiv:2109.07161*, 2021. 5
- [35] Christian Szegedy, Vincent Vanhoucke, Sergey Ioffe, Jon Shlens, and Zbigniew Wojna. Rethinking the inception architecture for computer vision. In *Proceedings of the IEEE conference on computer vision and pattern recognition*, pages 2818–2826, 2016. 5
- [36] Narek Tumanyan, Michal Geyer, Shai Bagon, and Tali Dekel. Plug-and-play diffusion features for text-driven image-to-image translation. *arXiv preprint arXiv:2211.12572*, 2022. 2, 15
- [37] Dani Valevski, Matan Kalman, Yossi Matias, and Yaniv Leviathan. Unitune: Text-driven image editing by fine tuning an image generation model on a single image. *arXiv preprint arXiv:2210.09477*, 2022. 2, 4
- [38] Su Wang, Chitwan Saharia, Ceslee Montgomery, Jordi Pont-Tuset, Shai Noy, Stefano Pellegrini, Yasumasa Onoe, Sarah Laszlo, David J. Fleet, Radu Soricut, Jason Baldridge, Mohammad Norouzi, Peter Anderson, and William Chan. Imagen editor and editbench: Advancing and evaluating text-guided image inpainting. *arXiv preprint arXiv:2212.06909*, 2023. 3
- [39] Chen Henry Wu and Fernando De la Torre. Unifying diffusion models’ latent space, with applications to cyclediffusion and guidance. *arXiv preprint arXiv:2210.05559*, 2022. 2
- [40] Hang Yu, Yufei Xu, Jing Zhang, Wei Zhao, Ziyu Guan, and Dacheng Tao. Ap-10k: A benchmark for animal pose estimation in the wild. In *Thirty-fifth Conference on Neural Information Processing Systems Datasets and Benchmarks Track (Round 2)*, 2021. 5, 12
- [41] Jiahui Yu, Zhe Lin, Jimei Yang, Xiaohui Shen, Xin Lu, and Thomas S Huang. Generative image inpainting with contextual attention. In *CVPR*, 2018. 3
- [42] Jiahui Yu, Zhe Lin, Jimei Yang, Xiaohui Shen, Xin Lu, and Thomas S Huang. Free-form image inpainting with gated convolution. In *ICCV*, 2019. 3
- [43] Yu Zeng, Zhe Lin, and Vishal M Patel. Shape-guided object inpainting. *arXiv preprint arXiv:2204.07845*, 2022. 3
- [44] Shengyu Zhao, Jonathan Cui, Yilun Sheng, Yue Dong, Xiao Liang, Eric I Chang, and Yan Xu. Large scale image completion via co-modulated generative adversarial networks. 2021. 3

Supplementary Material

In Appendix A we include a qualitative comparison with concurrent structure preserving methods, demonstrating how these methods often edit objects unmentioned by the text prompt. In Appendix B we discuss details regarding the MS-COCO ShapePrompts benchmark, in Appendix C we discuss details regarding our annotator evaluation, and in Appendix D we report additional ablations. Finally, we show a variety of additional examples from our method including success and failure cases in Appendix E as well as inferred shape edits, inter-class edits, outside edits, and simultaneous inside-outside edits in Appendix F.

A. Qualitative Comparison with Concurrent Structure Preserving Methods

We compare our method with concurrent work listed in Table 1 of the main text (see Figure 14). We can see that our method is able to perform better localized edits on a real image. Because these methods lack an explicit shape, they often change irrelevant objects that are not specified in the text prompt. In Row 2, Col 1-3 not only is the horse transformed into a robot but also the man. In Row 5, Col 3-4 the hanging plants and horse in the real image are merged into a horse with an entirely new pose. In Row 6, Col 3, 5 the wall that was present in the real image disappears. In contrast, the variant of our method that uses automatically inferred shapes (thereby requiring the same amount of input as the structure preserving methods) is able to perform edits that only modify the object of interest without disturbing the background. We used the official codebases released by the respective baselines and generated results using their default hyperparameter settings.

B. MS-COCO ShapePrompts Details

Prompts For our MS-COCO ShapePrompts benchmark we design a set of prompts where it is possible to simultaneously synthesize an object that is shape faithful and text aligned (as opposed to prompts entangled with shape, i.e., transforming “chihuahua dog” to “poodle dog” while respecting shape is difficult because poodles are characterized by floppy ears and fluffy fur). While our method is able to perform inter-class edits as seen in Figure 8, we focus our experiments on intra-class edits which make more sense given the shape constraint (e.g. some hyper-specific shapes like the silhouette of an elephant only make sense when edits are done within the object class). For this reason we design prompts for each object class as seen in Figure 9. These prompts were inspired by examples from prior work [1, 8] and a search engine with paired prompts and synthetic images from Stable Diffusion [29].

Shape Faithfulness Metric To measure shape faithfulness we use the pretrained segmentation model MaskFormer

```
prompts = {
  "bear": [
    "stuffed {}",
    "{} wearing sunglasses"
  ],
  "bird": [
    "{} with blue and yellow feathers",
    "{} with iridescent feathers"
  ],
  "cat": [
    "spotted leopard {}",
    "{} wearing a yellow and black tie"
  ],
  "dog": [
    "{} wearing a floral jacket",
    "{} wearing a colorful shirt"
  ],
  "elephant": [
    "{} wearing christmas decorations",
    "holi festival {}"
  ],
  "horse": [
    "futuristic biomechanical robotic {} with synthetic body parts showing",
    "{} covered with gold and diamond chains"
  ],
  "sandwich": [
    "tortilla wrapped {}",
    "{} with peanut butter and jelly filling"
  ],
  "boat": [
    "inflatable {}",
    "{} made of candies"
  ],
  "kite": [
    "origami {} made of paper",
    "glitter {}"
  ],
  "truck": [
    "lego {}",
    "{} with spray paint graffiti"
  ],
}
```

Figure 9: Prompts from the MS-COCO ShapePrompts benchmark.



Figure 10: Synthetic images and their corresponding predicted segmentation and mIoU. Out-of-distribution variants of the object class, such as a truck made of legos, are still segmented correctly.

[4]. We demonstrate that the model makes meaningful predictions on synthetic images in Figure 10. Even more, the model’s predictions are reasonably robust to out-of-distribution variants of the object class, such as “lego truck.”

Approach	Guidance Scale	KW-mIoU	mIoU (\uparrow)	FID (\downarrow)	CLIP (\uparrow)
Real Images	N/A	86.5	78.6	-	0.16
(1) SD	7.5	30.9	52.5	46.2	0.21
(2) SD + DDIM Inv	7.5	39.8	61.2	42.8	0.21
(3) SD + DDIM Inv + Re-Weight (Ours w/o IOA)	3.5	46.2	59.6	40.6	0.21
(4) SD + DDIM Inv + Re-Weight + Token Inside-Outside Attn	3.5	48.1	62.9	40.6	0.21
(5) SD + DDIM Inv + Re-Weight + Soft Inside-Outside Attn	3.5	51.4	66.2	40.2	0.21
(6) SD + DDIM Inv + Re-Weight + Hard Inside-Outside Attn (Ours)	3.5	54.8	67.6	39.0	0.21

Table 3: Ablations on MS-COCO ShapePrompts (validation set).

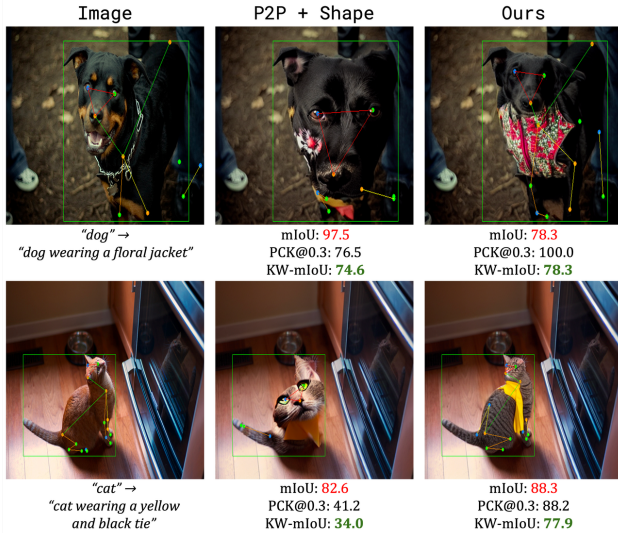


Figure 11: Comparison between mIoU and Keypoint-Weighted mIoU (KW-mIoU). Note that in this example P2P [8] receives a high mIoU score even though the edited objects are incorrectly scaled or cut off. By weighting each sample’s mIoU with the percentage of correct keypoints (PCK) to compute the KW-mIoU, we can measure shape faithfulness more reliably.

We use the segmentation model to compute mean intersection over union (mIoU). We compute mIoU on a per-sample basis (i.e., we average the IOU of each object regardless of size) as opposed to a per-pixel basis (which is typically used in semantic segmentation works) since it is equally important to synthesize both small and large objects in a shape-faithful fashion. We set all pixels outside the mask to a null prediction to compute mIoU only within the edited mask region. We do this because in some settings (e.g. MS-COCO instance masks) the mask may specify one object instance out of multiple to edit, but our segmentation model would identify all instances of the same category, which would result in a diluted mIoU score. Additionally, for all methods that use “copy background” the background should remain identical to the original image.

In addition to mIoU, we introduce a new metric called Keypoint-Weighted mIoU (KW-mIoU). One issue with the

standard mIoU metric is that edited objects that are incorrectly scaled or cut off could still get a very high mIoU if they fully occupy the shape (see Figure 11, Col 2). In order to mitigate this issue, we report KW-mIoU for animal classes (horse, dog, cat, elephant) where we weight each sample’s mIoU by the percentage of correct keypoints (PCK) as computed between the source and edited images. We report KW-mIoU for animal classes only as we were not able to find a robust object pose estimation model with open-vocabulary capacities and reliable performance. By incorporating pose information, the proposed metric is able to be more sensitive to scale and object parts, and thus measure shape faithfulness more reliably. We use an animal keypoint detection model HRNet [33] pretrained on AP-10K dataset [40] as provided by <https://github.com/open-mmlab/mmpose>.

C. Annotator Evaluation Details

Our annotator evaluation included 25 total people spread across 5 evaluations (Ours vs. Blended Diffusion, Ours vs. SD-Inpaint, Ours vs. SDEdit + Shape, Ours vs. P2P + Shape, Ours vs. P2P vs. P2P + Shape). We asked each annotator to rate 100 samples, where they were told that they would be “rating AI-edited images, where the goal is to edit one object according to a text prompt while maintaining its shape.” Each sample was formatted as pictured in Figure 12, in the grid the first column (“Original”) corresponds to the original image, the second column (“A”) corresponds to an edited image, and the third column (“B”) corresponds to another edited image. To help annotators judge faithfulness in addition to the first row (“Full Image”) we also provide the second row (“Masked Object”) which masks the full image according to the shape of the original object. Along the metrics of shape faithfulness, text alignment, and image realism we asked annotators to rate whether synthetic image A or B performed better, or whether they “Tie.” We define the metrics using the instructions seen in Figure 13.

We also gave annotators the option to mark whether one of the synthetic image makes no substantial edit to the original object (i.e. the image copies and recolors the same object), which would be unfairly marked as having better shape faithfulness and image realism at the cost of text

dog wearing a floral jacket

	Original	A	B
Full Image			
Masked Object			

In which image does the object best match the shape? *

☒ A
☐ B
☐ Tie

In which image does the object best match the text description? *

☒ A
☐ B
☐ Tie

In which image does the object have the best realism and quality? *

☒ A
☐ B
☐ Tie

Figure 12: Screenshot of our annotator evaluation. People were asked to compare images edited by our method versus a baseline in anonymized and randomized order and rate (1) shape faithfulness, (2) text alignment, (3) image realism. In our final evaluation comparing Ours vs. P2P vs. P2P + Shape they also rated (4) best overall edit.

alignment under our evaluation standard. We removed these marked samples from our final comparison, resulting in the removal of less than 10% of samples from the 2500 total samples (from 25 annotators rating 100 images each) across all evaluations.

D. Additional Ablations

We report an ablation study in Table 3. (1) uses a standard guidance scale of 7.5 and copies the background of the

1. Shape

Definition: The edited object matches the scale and silhouette of the original object, and it is not cut off, zoomed out, or zoomed in. If the edited objects are similar in shape faithfulness, you may tie-break by judging the pose.

Heuristic: The edited object fills the masked version of the image in the "Masked Object" row.

2. Text

Definition: The edited object matches the text prompt.

Heuristic: The edited object matches what you were imagining given the text prompt.

3. Realism

Definition: The edited image looks realistic and lacks visual artifacts or logical flaws.

Heuristic: If you saw it on the internet you would believe the image is a real photograph / created by a human artist.

4. Best Edit

Definition: The edited image is the best along all three axes.

Heuristic: The edited image is what you would expect if a human were to edit the original image in Photoshop, i.e. most of the content is similar to the original image except the object which is modified according to the text prompt.

Figure 13: Metric definitions given as reference in the annotator evaluation.

real image onto the prediction at each timestep as done in Blended Diffusion [1], (2) uses DDIM inverted noise during the generation process, (3) re-weights cross-attention maps based on the change between \mathcal{P}_{src} and \mathcal{P}_{edit} as done in P2P [8]¹, (4) applies Inside-Outside Attention only to the cross-attention layers (Token Inside-Outside Attn), (5) applies Inside-Outside Attention with a hard mask for the cross-attention and soft mask for the self-attention layers (Soft Inside-Outside Attn), and (6) applies Inside-Outside Attention with a hard mask for both the cross- and self-attention layers (Hard Inside-Outside Attn), the design used in our final method. Comparing (1) and (2), we show that using DDIM inverted noise helps in both mIoU and FID. For (3), we empirically find that higher guidance scale, when used in combination with DDIM inversion, makes the model rely less on the the inverted noise, resulting in less realistic editing. However, we find that simply lowering the guidance scale leads to degradation in text faithfulness. Using cross-attention re-weighting mitigates this issue and allows us to achieve better image realism with similar performance in shape and text faithfulness. In (4), when we apply the Inside-Outside Attention mechanism only to the cross-attention layers we observe a small boost in mIoU with the same FID score, and when we apply it to both the cross- and self-attention layers in (5) we observe a more significant boost of 6.6 points in mIoU and 0.4 points in FID from (3). Comparing (5) and (6) we find that using a hard mask for Inside-Outside Attention performs better than using a soft mask, as seen by the further boost of 1.4 points in mIoU and 1.2 points in FID. Our final method that combines DDIM inversion, re-weighting, and hard Inside-Outside Attention achieves the best performance in mIoU and FID with scores of 67.6 and 39.0 respectively without a degradation in CLIP score.

¹When re-weighting, we use a constant scalar upweighting of 2.5 as determined by hyperparameter sweeps in early experiments.

E. Success / Failure Cases

Success Cases In Figure 16 we show edits made by our method for each prompt in the MS-COCO ShapePrompts benchmark. We demonstrate that our method is able to handle partially occluded masks and maintain relationships between the object and background, as seen in the case of the “inflatable boat” where the edit maintains the position of the man and dog on that boat. We demonstrate that our method is able to add accessories while simultaneously respecting the input shape, as seen by the “elephant wearing christmas decorations” where an ear is converted to a santa hat. Finally, our method is seamlessly able to edit material (“lego truck”, “boat made of candies”, “origami kite made of paper”) and color (“truck with spray paint graffiti”, “bird with iridescent feathers”, “holi festival elephant”).

Failure Cases We also show failure cases of our method in Figure 17. Sometimes the shape is inherently difficult, such as the case with (a) uncommon pose (i.e., our method repositions an elephant sitting on its hind legs to standing), (b) uncommon perspective (i.e., our method transforms a close-up of a dog’s eyes to a dog’s entire face and converts its hair into fabric to obey the “floral jacket” in the prompt), or (c) multi-part mask inputs (i.e., our method only edits the front half of the truck into a lego material). Since we use DDIM inversion (d) ghosting can occur where remnants of the original object (e.g. a mouth or ear) can appear in the synthesized object. Since we localize the attention maps (e) global context can be ignored (i.e., our method edits a colorful dog into a black-and-white photo or creates artifacts at the boundary between a dog’s legs and water). Finally, our method may produce strange (f) accessory placement (i.e., our method places a bowtie on the cat’s arm because its neck is not visible in the original image).

F. Additional Editing Results

Inferred Shape Edits Building on Figure 1 and our discussion in Sec. 5.1, we show additional examples of edits made by our method with an inferred shape as input in Figure 15. Our method is able to handle a wide array of inferred shapes including those with multiple instances, noise, and occlusions.

Inter-Class Edits Building on our discussion in Section Sec. 5.2, we show additional examples of inter-class edits in Figure 18, including converting from cat to dog, dog to cat, or sheep to cow.

Outside Edits. We show additional examples of outside edits in Figure 19, including transforming the background to different locations, seasons, or times of day.

Simultaneous Inside-Outside Edits We show additional examples of simultaneous inside-outside edits in Figure 20, including transporting a dog to different fictional locations from Star Wars and The Hobbit or a cat to a coral reef

and beach, while maintaining their shape relationship to the background based on the input mask.

Spurious Attentions and Classifier-Free Guidance

In Sec. 3 we discuss how our Inside-Outside Attention mechanism is able to better perform reconstruction and editing with classifier-free guidance by removing spurious attentions. We additionally show our method vs. P2P [8] in the same setting in Figure 21. P2P exhibits spurious attentions where the token “dog” not only attends to the dog but also the background, causing the shape of the original dog to diverge completely.

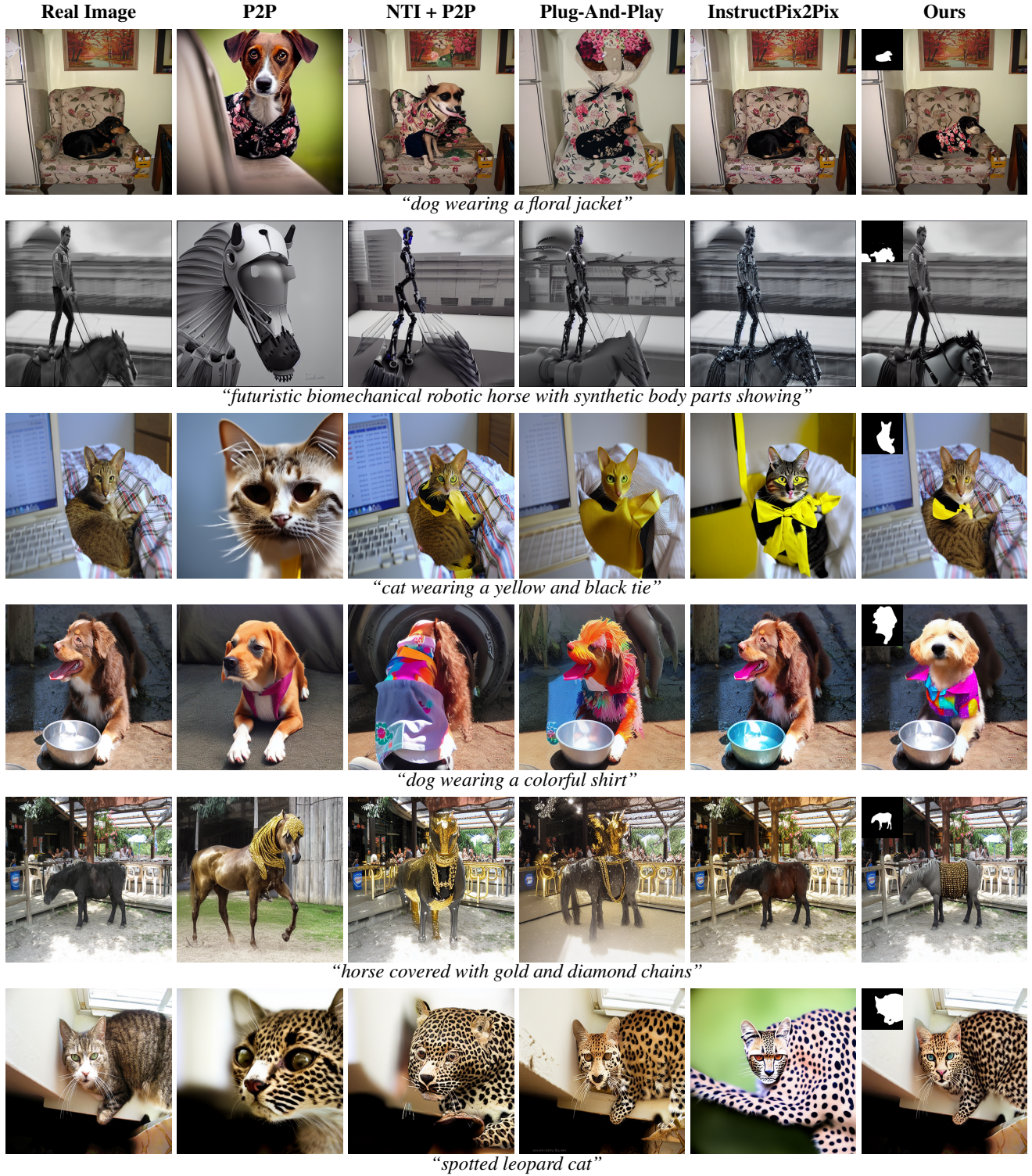


Figure 14: Qualitative examples comparing our method with concurrent work for structure preserving editing. We compare against P2P [8], NTI + P2P [20], Plug-and-Play [36], and InstructPix2Pix [2]. Here, we use the variant of our method that uses inferred shape (pictured in the top left corner), which requires the same amount of input (real image and text prompts) as the structure preserving methods.



Figure 15: Additional examples generated by our method with masks automatically inferred from the text (predicted by MaskFormer [4]). Depending on the inferred shape, our method is able to edit multiple instances and handle complex shapes caused by noisy mask predictions or severe occlusions.

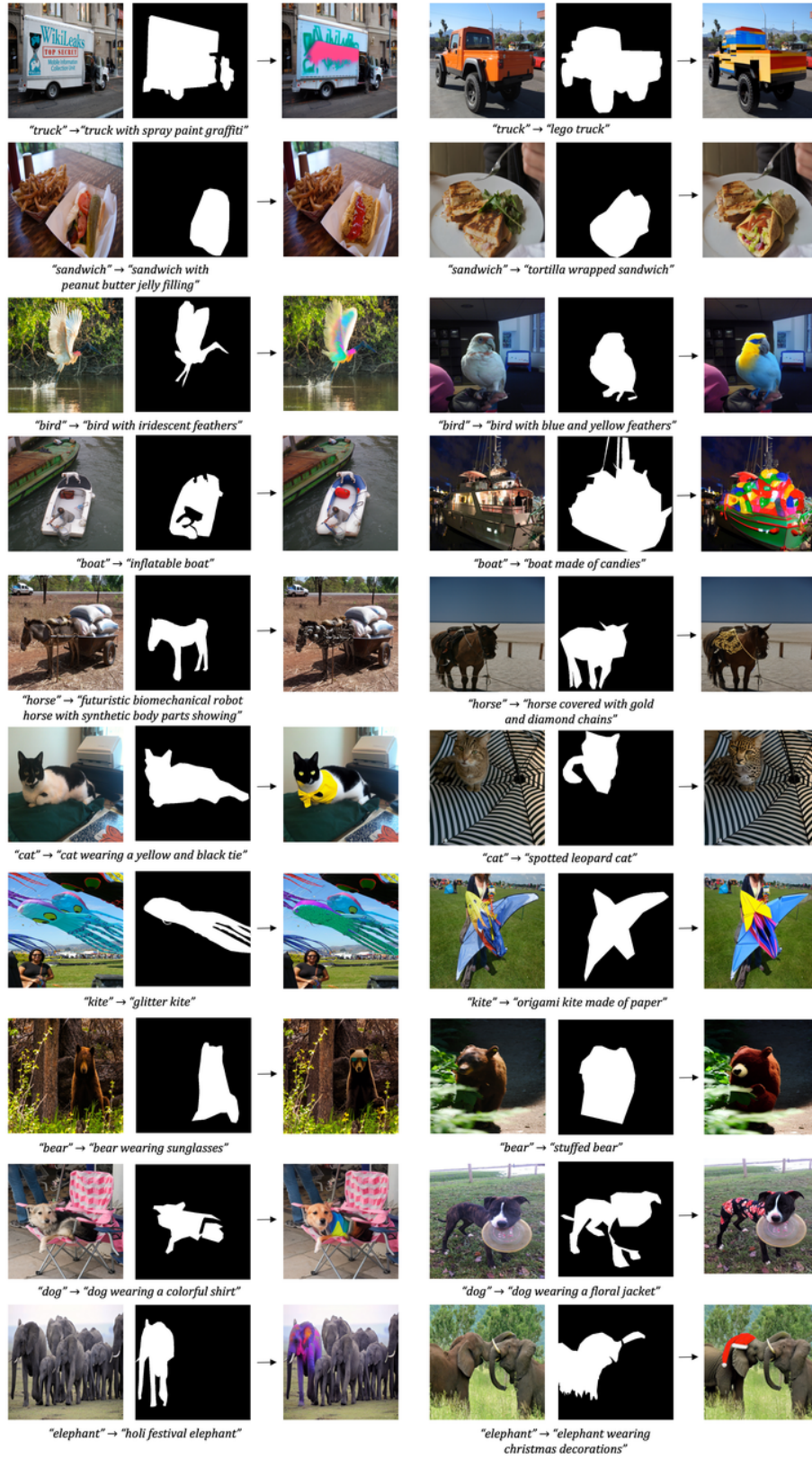


Figure 16: Examples of success cases from our method that demonstrate its ability to handle partially occluded masks, add accessories, transform materials, or recolor objects.



Figure 17: Examples of failure cases from our method that relate to (a) uncommon pose, (b) uncommon perspective, (c) multi-part mask, (d) ghosting, (e) global context, (f) accessory placement.

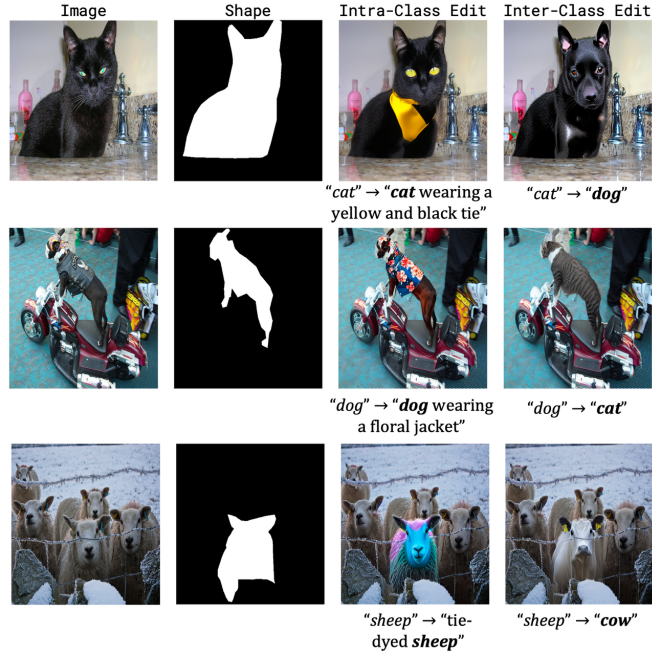


Figure 18: Additional examples of inter-class edits.



Figure 19: Additional examples of outside edits from our method where we transform the background to various locations (New York City, London), seasons (winter, autumn), and times of day (sunset, night) for various objects (truck, boat, cat).

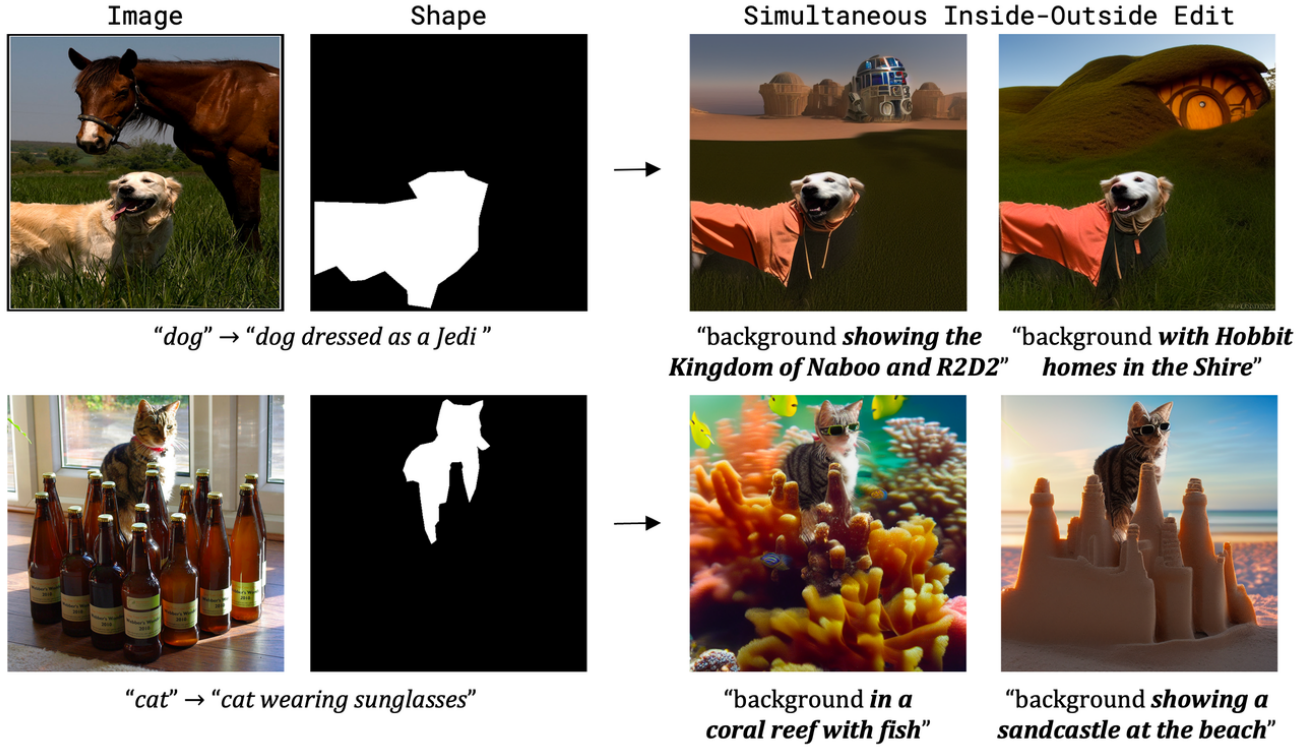


Figure 20: Additional examples of simultaneous inside-outside edits from our method where we transform both the object and background while maintaining the original shape relationship.

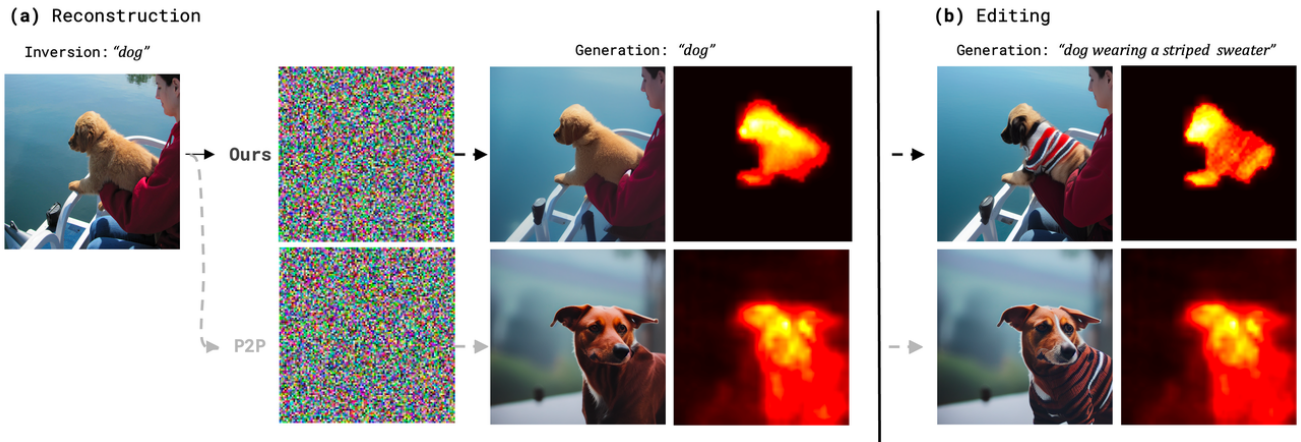


Figure 21: Spurious attentions and classifier-free guidance also affects P2P [8]. We compare our method (top) and P2P (bottom) for reconstructing (left) and editing (right) an image with corresponding cross attention maps for the token "dog" averaged over all layers and timesteps.